Research Article Vol. 60, No. 29 / 10 October 2021 / Applied Optics 9249

applied optics

3–6 μm dispersive mirrors compensating for dispersion introduced by the GaAs crystal

Yu Chen,[1,2] Daniel Hahner,[1] and Vladimir Pervak[1,*]

[1]Ludwig-Maximilians-Universitaet Muenchen, Am Coulombwall 1, 85748 Garching, Germany
[2]Max-Planck Institute of Quantum Optics, Hans-Kopfermann Str. 1, 85748 Garching, Germany
*Corresponding author: vladimir.pervak@physik.uni-muenchen.de

Received 27 August 2021; revised 22 September 2021; accepted 24 September 2021; posted 27 September 2021 (Doc. ID 441787); published 8 October 2021

A new broadband dispersive mirror (DM), which consists of Si and SiO_2 layer materials operating in the spectral range of 3–6 μm, is developed for the first time, to our knowledge. The DM is able to compensate for the dispersion of a 0.5 mm thick GaAs crystal per bounce. Pulse analysis proves that the compensation effect of the DM is much better than a CaF_2 plate, which is the commonly used dispersion compensation element in mid-infrared optical parametric oscillators (MIR OPOs), and the new MIR DM could improve the MIR OPO spectrum with better pulse quality and short pulse duration.

https://doi.org/10.1364/AO.441787

1. INTRODUCTION

Dispersive mirrors (DMs), which provide precise group delay dispersion (GDD) compensation, have been successfully used in the visible [1–3] and near-infrared ranges [4–9]. It includes Ti:Sa lasers [1–3], Yb:YAG lasers [4,5], erbium-doped fiber lasers [6], and Cr:ZnS/Cr:ZnSe lasers [7–9]. DMs in this range have been improved further and further and are now commercially available. The mid-infrared (MIR) fingerprint region where molecules have their distinct absorption features associated with ro-vibrational transitions is critical for high-resolution spectroscopy, trace molecular sensing, and chemical standoff detection [10,11]. As more scientists are attracted towards MIR laser systems, the demand of corresponding dispersion compensation elements is growing. Broadband DMs operating in the spectral range from 6.5 to 11.5 μm were successfully developed and applied in a broadband MIR field resolving spectrometer [12]. In [13], a DM providing a group delay (GD) variation of 60 fs with an average reflectance of 97.5% in the spectral range from 9 to 11.5 μm was synthesized. DMs in this region have become a key element to compensate for dispersion.

The extension of the frequency comb to the MIR enables exciting applications such as coherent molecular spectroscopy and trace gas detection [14], attosecond physics [15], and laser-driven particle acceleration [16]. Optical parametric oscillators (OPOs) are one of the key components to realize the extension of the frequency comb to the MIR fingerprint region. An orientation-patterned (OP)-GaAs crystal, which has a large second-order nonlinear optical coefficient and good MIR transparency, makes it very suitable for MIR optical parametric frequency conversion. However, to the best of our knowledge, in most of the published works [17–20], the dispersion of the GaAs crystal was compensated for by CaF_2 or YAG plates. The dispersion was not perfectly compensated for, which limits the achievable pulse duration and spectral bandwidth [17–19].

In this work, for the first time, a new DM composed of Si and SiO_2 layers, which can compensate for the dispersion of a 0.5 mm GaAs crystal in the spectral range of 3–6 μm, was designed, fabricated, and characterized. The refractive indices of Si and SiO_2 were determined by measuring transmission and reflection spectra of the single layers and quarter-wave multilayer. The design and production of the MIR DM are shown in Section 2. In Section 3, the characterization of the DM and pulse simulations compared to the CaF_2 are described. We draw our conclusions in Section 4.

2. DESIGN AND PRODUCTION

To design a MIR DM spanning over one octave, which could compensate for the dispersion introduced by a 0.5 mm GaAs crystal, a proper material combination must be chosen. As we know, due to the relatively low refractive index ratio and absorption problem, the widely used thin film materials for visible and near-infrared ranges is no longer suitable for the MIR range. Si and SiO_2 with a higher refractive index ratio of about 2.3 have proven to be very successful in a 2–4 μm DM [7,8]. In this paper, Si and SiO_2 were considered as the high and low index materials, respectively.

The refractive indices of Si and SiO_2 were determined from single Si and SiO_2 layers as well as a Si/SiO_2 quarter-wave mirror. The single Si layer was deposited on a fused silica substrate with a temperature of 180°C. After production, the transmittance, reflectance, and back side reflectance were measured by a

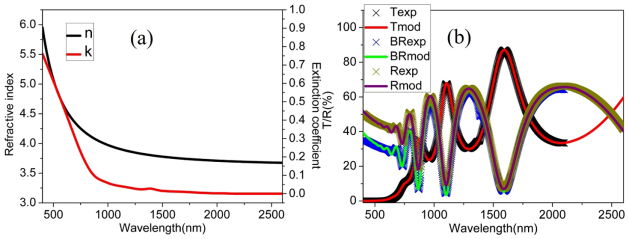

Fig. 1. (a) Determined optical constant of Si layer and (b) fitting of measured transmittance and reflectance data of Si layer by the model data.

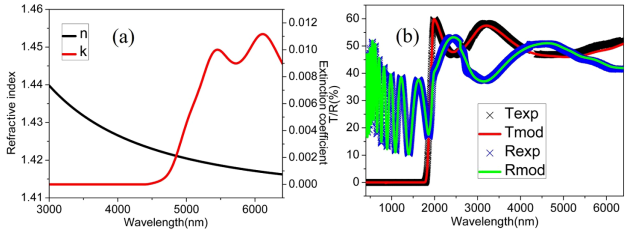

Fig. 2. (a) Determined optical constant of SiO_2 layer and (b) fitting of measured transmittance and reflectance data of SiO_2 layer by the model data.

Perkin Elmer Lambda 950 spectrophotometer. The refractive index was determined by the well-known Cauchy model

$$n(\lambda) = n_\infty + A/\lambda^2 + B/\lambda^4, \tag{1}$$

where λ is expressed in micrometers, n_∞ is a dimensionless parameter, A and B are in units of μm^2 and μm^4, respectively, and the extinction coefficient is defined by the non-parameter approach [21] based on the following discrepancy function:

$$\mathrm{DF}^2 = \sum_{j=1}^{L} \left\{ S\left(n(\lambda_j), k(\lambda_j), d; \lambda_j\right) - S(\lambda_j) \right\}^2 + \alpha_1 \sum_{j=1}^{L} \left\{ n''(\lambda_j) \right\}^2 + \alpha_2 \sum_{j=1}^{L} \left\{ k''(\lambda_j) \right\}^2, \tag{2}$$

where $S(n(\lambda_j), k(\lambda_j), d; \lambda_j)$ is the theoretical spectral characteristic of the sample, $S(\lambda_j)$ is the measured spectral characteristic, $n''(\lambda_j)$ and $k''(\lambda_j)$ are the finite-difference second order derivatives of the refractive index and extinction coefficient, respectively, and α_1 and α_2 are weight parameters. Calculation of the refractive indices and extinction coefficient was performed with OptiRe software. The optical constants of Si are shown in Fig. 1(a). The Cauchy parameters are $n_\infty = 3.623242$, $A = 0.346575\ \mu m^2$, and $B = 4.1371427 \cdot 10^{-3}\ \mu m^4$. In Fig. 1(b), great agreement between the experimental data and model data can be observed.

The single SiO_2 layer was deposited on a Ge substrate with a temperature of 180°C. The transmittance and reflectance were measured by the Perkin Elmer Lambda 950 spectrophotometer in the wavelength range from 400 to 2600 nm. The spectra beyond 2600 nm were measured by a Bruker Fourier Transform Infrared spectrometer (FTIR, Vertex 70, Bruker Optics GmbH). The dispersion behavior of the SiO_2 refractive index was described by the Cauchy model, and the extinction coefficient was described by the non-parameter approach. The optical constants are plotted in Fig. 2(a). The Cauchy coefficients are 1.409599, $0.271791\ \mu m^2$, and $1.3099339 \cdot 10^{-4}\ \mu m^4$, respectively. The experimental data show great agreement with the model data, as presented in Fig. 2(b).

A quarter-wave mirror with a central wavelength of 4100 nm was deposited on a fused silica substrate with a temperature of 180°C to calibrate the deposition rates and verify the refractive indices in the multilayer structure. The reflectance was recorded by a FTIR spectrometer. Based on the OptiRe software [22], the deposition rates were calibrated by reverse engineering. The experimental reflectance compared to the model reflectance is presented in Fig. 3. A good correspondence between the measurement and the model was obtained.

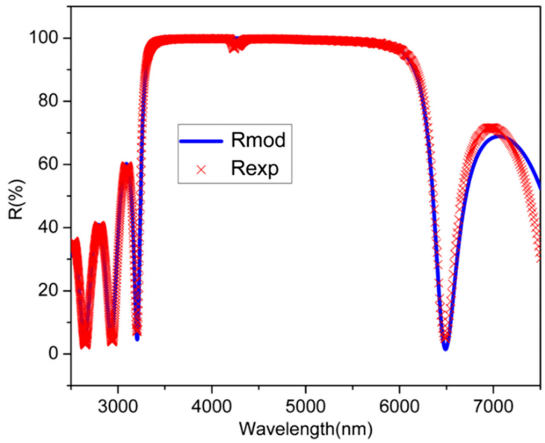

Fig. 3. Correspondence between the experimental and model reflectance.

After determining the refractive indices of both materials, we started to design the DM. The OptiLayer software [22] with powerful needle optimization and gradual evolution algorithms was used in the design process. The reflectance and GD were chosen as the target characteristics. The target GD was the GD of a 0.5 mm GaAs crystal with the opposite sign and shifting in the vertical direction, while the target reflectance was 100%. The target GD value at the wavelength of 4500 nm is 59 fs and the GD difference between 3000 and 6000 nm is about 60 fs. The merit function was defined as

$$\mathrm{MF}(X)^2 = \sum_{j=1}^{520} \left(\frac{R(X, \lambda_j) - R(\lambda_j)}{\Delta R_j} \right)^2 + \sum_{j=1}^{520} \left(\frac{\mathrm{GD}(X, \lambda_j) - \mathrm{GD}(\lambda_j)}{\Delta \mathrm{GD}_j} \right)^2, \tag{3}$$

where $\{\lambda_j\}$ are distributed wavelength points in the spectral range of 3000–6000 nm, $X = (d_1, \ldots, d_m)$ is the vector of the layer thicknesses, and m is the layer number; $R(X, \lambda_j)$ and $\mathrm{GD}(X, \lambda_j)$ are the actual reflectance and GD, $R(\lambda_j)$ and $\mathrm{GD}(\lambda_j)$ are the reflectance and GD target, and ΔR_j and $\Delta \mathrm{GD}_j$ are the tolerance of reflectance and GD, respectively.

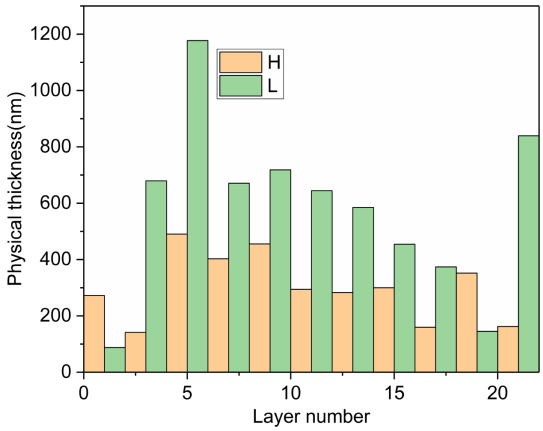

Fig. 4. Layer structure of the DM. Yellow and green bars represent high and low index materials, respectively. The layer number is starting from the substrate to the incident medium (air).

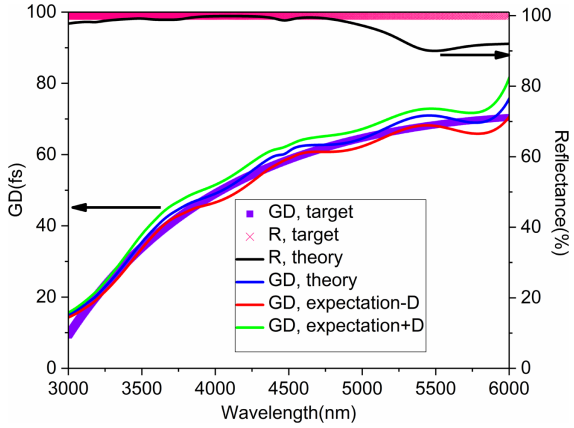

Fig. 5. Theoretical reflectance and GD. Pink cross and violet square represent R and GD targets; black and blue curves represent theoretical R and GD; and red and green curves represent the probability corridor for a 2% relative error and 2 nm absolute error, respectively.

A DM theoretically able to compensate for the dispersion of a 0.5 mm GaAs crystal per bounce was obtained after carefully adjusting the tolerance and optimizing the design. The layer structure is shown in Fig. 4. The total thickness is about 9.7 μm, which is not very thick considering that this mirror works in the MIR range. The theoretical reflectance, GD, as well as an error analysis are plotted in Fig. 5. Layer thicknesses were randomly varied with a relative error of 2% and an absolute error of 2 nm, which are much larger than the real deposition errors. For each design, we computed the GD and performed a statistical analysis of the obtained GD dependencies. The red and green curves in Fig. 5 define the border of errors that encloses GD values with a probability of 68.3%. Based on the computational error analysis, we could study the sensitivity of the DM to deposition errors. Figure 5 shows that even with a 2% relative error and a 2 nm absolute error, the GD curves have only a small deviation from the theoretical GD curve and fit well with the GD target. This means the DM is quite robust to layer thickness errors.

The 3–6 μm DM was fabricated with ion beam sputtering (Cutting Edge Coatings, Hannover, Germany). To reduce the absorption of both materials, the substrates were heated to 180° for 2 h before deposition by two quartz radiation heaters. The chamber was pumped down to 1×10^{-7} mbar by a cryogenic pump. The argon gas plasma was generated by a radio-frequency ion source. Both Si and SiO_2 were sputtered from a silicon target with a purity of 99.999%. During the Si layers, no oxygen was added to the coating chamber. For the SiO_2 layers, the amount of 90 standard cubic centimeters per minute (sccm) was ejected near the pure Si target. The thickness was controlled by a well-calibrated time control technique. The deposition rates for Si and SiO_2 were 0.13 nm/s and 0.15 nm/s, respectively.

3. CHARACTERIZATION AND DISCUSSION

After deposition, reflectance data were measured by the FTIR in the wavelength range from 2500 to 6500 nm. Comparison between measured and theoretical reflectance is shown in Fig. 6. The reflectance degradation around 4300 nm is due to water absorption. It should be noted that this water absorption dip does not affect the phase performance of the laser system [12]. In addition, the water absorption around 5.1 μm does not affect the GD and GDD measurement. The GD and GDD were recorded by a MIR white light interferometer built in-house [23], which is also based on the FTIR. The measured

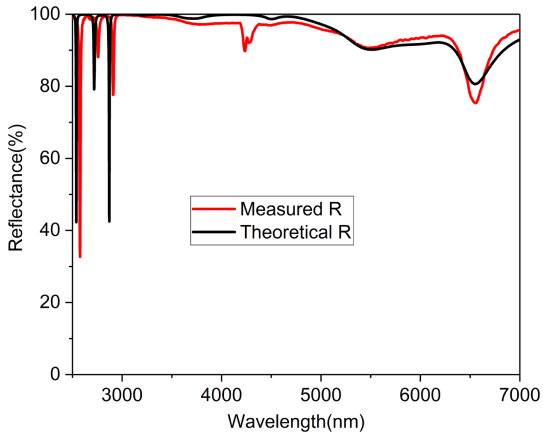

Fig. 6. Comparison between the measured and theoretical reflectance. Black and red curves correspond to the measured and theoretical reflectance, respectively.

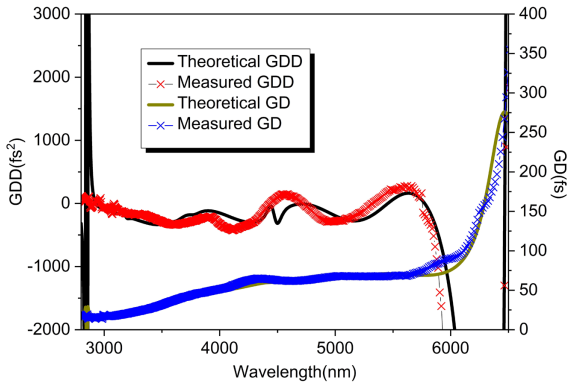

Fig. 7. Comparison between measured and theoretical GD and GDD. Yellow and black curves represent the theoretical GD and GDD, and blue and red crosses correspond to the measured GD and GDD, respectively.

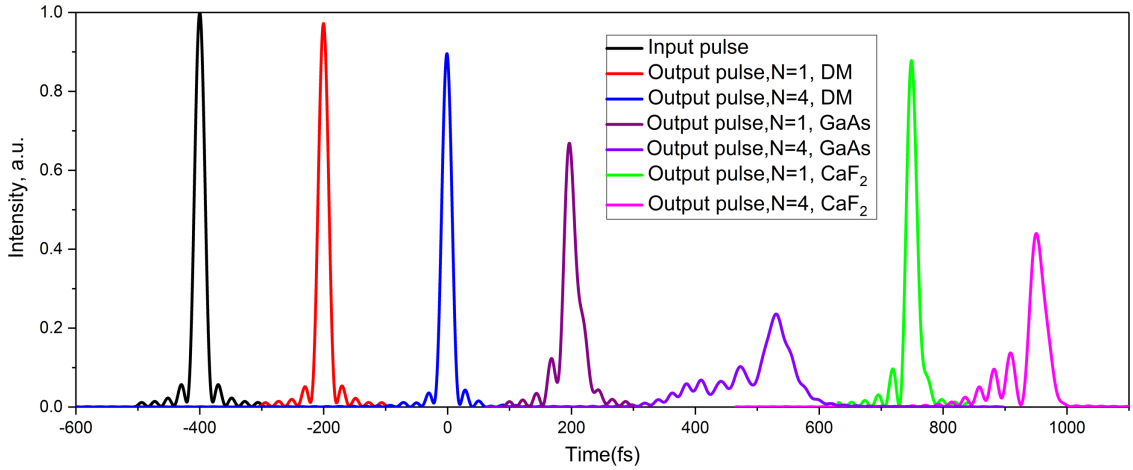

Fig. 8. Simulated input and output pulses. Black curve represents the input pulse. Red and blue curves correspond to output pulses reflected from the DM with one and four bounces, respectively. Purple and violet curves correspond to output pulses passing through a 0.5 mm thick GaAs crystal one and four times, respectively. Green and pink curves correspond to output pulses compensated for by 0.3 mm CaF_2 one and four times, respectively.

GD and GDD compared to the theoretical values are plotted in Fig. 7. A good agreement between the measured and theoretical GD and GDD data can be observed. The measured GD and GDD curves fit very well with the theoretical ones. Especially for the GD curves, the steep increase beyond 6 μm and the GD difference between 3 and 6 μm of about 60 fs could be measured.

To compare the compensation effect between the MIR DM and CaF_2, which is commonly used to compensate for the dispersion of GaAs, we simulated the envelopes of input and output pulses, which are compensated for by the DM and CaF_2, respectively. During the simulations, we assume that the input pulse is a Fourier transform limited pulse with a pulse duration of 18.8 fs and a full width at half maximum (FWHM) of 500 THz covering 3–6 μm. The input pulse first went through a 0.5 mm thick GaAs crystal. The stretched pulse was compressed by the DM and a 0.3 mm thick CaF_2. The simulated input pulse and output pulse are shown in Fig. 8.

From the simulations, we could see that the pulse duration and pulse shape do not change at all after one and four bounces from the DM (blue and red curves in Fig. 8). The pulse durations of both output pulses are about 18.9 fs and quite close to the transform limited pulse duration. The pulse intensity drops about 10% after four bounces from the DM, which corresponds to a total efficiency of 90%. Additionally, there are no satellites observed. On the contrary, the pulse shape compressed by CaF_2 has changed significantly after passing one and four times through it (green and pink curves in Fig. 8). The pulse durations increased to 19.4 and 29.2 fs after one and four times through the CaF_2, respectively. The intensity of the main pulse decreased drastically due to the appearance of the satellites. What is worse, the more times passing through the CaF_2, the longer pulse duration and worse pulse quality. These simulations have proven that the dispersion introduced by the GaAs crystal could be perfectly compensated for by the DM, while the compensation effect from the CaF_2 plate is much worse than the DM.

4. CONCLUSION

A new broadband DM that can perfectly compensate for the dispersion of a 0.5 mm GaAs crystal in the spectral range of 3–6 μm has been successfully designed and produced by ion beam sputtering for the first time. Pulse simulations show that the compensation effect of the DM is much better than the commonly used CaF_2 plates. This new type of DM could perfectly compensate for the dispersion of a GaAs crystal, which will benefit the MIR OPO output spectrum, including better pulse quality and shorter pulse duration.

Funding. Munich-Centre for Advanced Photonics.

Acknowledgment. The authors thank Prof. Ferenc Krausz for valuable discussion and permanent support of this work.

Disclosures. The authors declare no conflicts of interest.

Data Availability. Data underlying the results presented in this paper are not publicly available at this time but may be obtained from the authors upon reasonable request.

REFERENCES

1. V. Pervak, C. Teisset, A. Sugita, S. Naumov, F. Krausz, and A. Apolonski, "High-dispersive mirrors for femtosecond lasers," Opt. Express **16**, 10220–10233 (2008).
2. P. Dombi, P. Rácz, M. Lenner, V. Pervak, and F. Krausz, "Dispersion management in femtosecond laser oscillators with highly dispersive mirrors," Opt. Express **17**, 20598–20604 (2009).
3. R. Chen, Y. Wang, K. Guo, Y. Zhang, Z. Wang, M. Zhu, K. Yi, Y. Leng, and J. Shao, "Angle-adjustment-based tunable chirped mirrors with continuous dispersion compensation," Opt. Lett. **44**, 6053–6056 (2019).
4. E. Fedulova, K. Fritsch, J. Brons, O. Pronin, T. Amotchkina, M. Trubetskov, F. Krausz, and V. Pervak, "Highly-dispersive mirrors reach new levels of dispersion," Opt. Express **23**, 13788–13793 (2015).
5. O. Pronin, J. Brons, C. Grasse, V. Pervak, G. Boehm, M.-C. Amann, A. Apolonski, V. L. Kalashnikov, and F. Krausz, "High-power Kerr-lens mode-locked Yb:YAG thin-disk oscillator in the positive dispersion regime," Opt. Lett. **37**, 3543–3545 (2012).

6. Y. Chen, Y. Wang, L. Wang, M. Zhu, H. Qi, J. Shao, X. Huang, S. Yang, C. Li, K. Zhou, and Q. Zhu, "High dispersive mirrors for erbium-doped fiber chirped pulse amplification system," Opt. Express **24**, 19835–19840 (2016).
7. V. Pervak, T. Amotchkina, Q. Wang, O. Pronin, K. Mak, and M. Trubetskov, "2/3 octave Si/SiO_2 infrared dispersive mirrors open new horizons in ultrafast multilayer optics," Opt. Express **27**, 55–62 (2019).
8. V. Pervak, T. Amotchkina, D. Hahner, S. Jung, Y. Pervak, M. Trubetskov, and F. Krausz, "Complementary Si/SiO_2 dispersive mirrors for 2-4 μm spectral range," Opt. Express **27**, 34901–34906 (2019).
9. T. Amotchkina, M. Trubetskov, F. Habel, Y. Pervak, J. Zhang, K. Mak, O. Pronin, F. Krausz, and V. Pervak, "Synthesis, fabrication and characterization of a highly-dispersive mirrors for the 2 μm spectral range," Opt. Express **25**, 10234–10240 (2017).
10. A. Schliesser, N. Picqué, and T. W. Hänsch, "Mid-infrared frequency combs," Nat. Photonics **6**, 440–449 (2012).
11. Z. Zhang, C. Gu, J. Sun, C. Wang, T. Gardiner, and D. Reid, "Asynchronous midinfrared ultrafast optical parametric oscillator for dual-comb spectroscopy," Opt. Lett. **37**, 187–189 (2012).
12. T. Amotchkina, M. Trubetskov, S. Hussain, D. Hahner, D. Gerz, M. Huber, W. Schweinberger, I. Pupeza, F. Krausz, and V. Pervak, "Broadband dispersive Ge/YbF3 mirrors for mid-infrared spectral range," Opt. Lett. **44**, 5210–5213 (2019).
13. F. Habel and V. Pervak, "Dispersive mirror for the mid-infrared spectral range of 9–11.5 μm," Appl. Opt. **56**, C71–C74 (2017).
14. F. Keilmann, C. Gohle, and R. Holzwarth, "Time-domain mid-infrared frequency-comb spectrometer," Opt. Lett. **29**, 1542–1544 (2004).
15. P. B. Corkum and F. Krausz, "Attosecond science," Nat. Phys. **3**, 381–387 (2007).
16. C. M. S. Sears, E. Colby, R. J. England, R. Ischebeck, C. McGuinness, J. Nelson, R. Noble, R. H. Siemann, J. Spencer, D. Walz, T. Lettner, and R. L. Byer, "Phase stable net acceleration of electrons from a two-stage optical accelerator," Phys. Rev. ST Accel. Beams **11**, 101301 (2008).
17. V. Smolski, S. Vasilyev, P. Schunemann, S. Mirov, and K. Vodopyanov, "Cr:ZnS laser-pumped subharmonic GaAs optical parametric oscillator with the spectrum spanning 3.6–5.6 μm," Opt. Lett. **40**, 2906–2908 (2015).
18. N. Leindecker, A. Marandi, R. Byer, K. Vodopyanov, J. Jiang, I. Hartl, M. Fermann, and P. Schunemann, "Octave-spanning ultrafast OPO with 2.6-6.1 μm instantaneous bandwidth pumped by femtosecond Tm-fiber laser," Opt. Express **20**, 7046–7053 (2012).
19. K. Vodopyanov, E. Sorokin, I. Sorokina, and P. Schunemann, "Mid-IR frequency comb source spanning 4.4–5.4 μm based on subharmonic GaAs optical parametric oscillator," Opt. Lett. **36**, 2275–2277 (2011).
20. V. Smolski, H. Yang, S. Gorelov, P. Schunemann, and K. Vodopyanov, "Coherence properties of a 2.6–7.5 μm frequency comb produced as a subharmonic of a Tm-fiber laser," Opt. Lett. **41**, 1388–1391 (2016).
21. T. Amotchkina, V. Janicki, J. Sancho-Parramon, A. Tikhonravov, M. Trubetskov, and H. Zorc, "General approach to reliable characterization of thin metal films," Appl. Opt. **50**, 1453–1464 (2011).
22. A. V. Tikhonravov and M. K. Trubetskov, "OptiLayer software," http://www.optilayer.com.
23. F. Habel, M. Trubetskov, and V. Pervak, "Group delay dispersion measurements in the mid-infrared spectral range of 2-20 μm," Opt. Express **24**, 16705–16710 (2016).